

Sonoluminescence as a QED vacuum effect

S. Liberati[†]

International School for Advanced Studies, Via Beirut 2-4, 34014 Trieste, Italy

F. Belgiorno[‡]

Università degli Studi di Milano, Dipartimento di Fisica, Via Celoria 16, 20133 Milano, Italy

Matt Visser[¶]

Physics Department, Washington University, Saint Louis MO 63130-4899, USA

D.W. Sciama[§]

International School for Advanced Studies, Via Beirut 2-4, 34014 Trieste, Italy

International Center for Theoretical Physics, Strada Costiera 11, 34014 Trieste, Italy

Physics Department, Oxford University, Oxford, England

(11 May 1998)

Schwinger has proposed a physical mechanism for sonoluminescence in terms of changes in the properties of the quantum-electrodynamic (QED) vacuum state during collapse of the bubble. This mechanism can be phrased in terms of the Casimir effect (static, quasi-static, or dynamic) and has recently been the subject of considerable discussion, debate, and controversy. The present paper extends this quantum-vacuum approach to sonoluminescence. We calculate Bogolubov coefficients relating the QED vacuum in the presence of the expanded bubble to that in the presence of the collapsed bubble. In this way we derive an estimate for the spectrum and total energy emitted. We emphasize the importance of the *difference* in refractive indices as a function of wavenumber, pressure, temperature, and noble gas admixture. Although the basic Casimir effect is a *universal* phenomenon of QED, specific and particular experimental features can be encoded in the refractive index.

I. INTRODUCTION

Sonoluminescence (SL) is the phenomenon of light emission by a sound-driven gas bubble in fluid [1]. The intensity of a standing sound wave can be increased until the pulsations of a bubble of gas trapped at a velocity node have sufficient amplitude to emit picosecond flashes of light with a “quasi-thermal” spectrum with a “temperature” of several tens of thousands of Kelvin. The basic mechanism of light production in this phenomenon is still controversial. We first present a brief summary of the main experimental data (as currently understood) and their sensitivities to external and internal conditions. The most common situation is that of an air bubble in water. For a more detailed discussion see [1].

Experiments of SL usually deal with bubbles of ambient radius $R_{ambient} \approx 4.5 \mu\text{m}$. The bubble is driven by a sound wave of frequency of 20–30 kHz. (Audible frequencies can also be used, at the cost of inducing deafness in the experimental staff.) During the expansion phase, the bubble radius reaches a maximum of order $R_{max} \approx 45 \mu\text{m}$, followed by a rapid collapse down to a minimum radius of order $R_{min} \approx 0.5 \mu\text{m}$. The photons emitted by such a pulsating bubble have typical wavelengths of the order of visible light. The minimum observed wavelengths range between 200nm and 100nm. This light appears distributed with a power law spectrum (with exponent depending on the noble gas admixture entrained in the bubble) with a cutoff in the extreme ultraviolet. If one fits the data to a Planck black-body spectrum the corresponding temperature is several tens of thousands of Kelvin (typically 70,000 K, though estimates varying from 40,000 K to 100,000 K are common). There is considerable doubt as to whether or not this temperature parameter corresponds to any real physical temperature. There are about one million photons emitted per flash, and the average total power emitted is $30 \text{ mW} \leq W \leq 100 \text{ mW}$. The photons appear to be emitted by a very tiny spatio-temporal region: of order $10^{-1} \mu\text{m}$ and on timescales $\tau \leq 50 \text{ ps}$.

A truly successful theory of SL must also explain a whole series of characteristic sensitivities to different external and internal conditions. Among these dependencies the main one is surely the mysterious catalytic role of noble gas admixtures. (Most often a few percent in the air entrained in the bubble. One can obtain SL from air bubbles with a 1% content of argon, and also from pure noble gas bubbles, but the phenomenon is practically absent in pure oxygen bubbles.)

Among other external conditions that influence SL we can quote: (1) Magnetic Fields — For fixed frequency of the driving sound wave $\hat{\nu}$, SL disappears above a pressure-dependent threshold magnetic field: $H \geq H_0(\hat{\nu})$, whereas for a fixed value of the magnetic field H_0 , the range of driving acoustic frequencies $\hat{\nu}$ for which SL exists is bigger than in the zero field case. This is often interpreted as suggesting that the primary effect of magnetic fields is to alter the condition for stable bubble oscillations. (2) Temperature of the water — If T_{H_2O} decreases then the emitted power W increases. The position of the peak of the spectrum depends on T_{H_2O} .

These are only the most salient dependencies of the SL phenomenon. In explaining such detailed and specific behaviour the Casimir approach (QED vacuum approach) encounters the same problems as other approaches have. Nevertheless we shall argue that SL explanations using a Casimir-like framework are viable. For instance, the presence of noble gas may vary solubilities of gas in the bubble, and this can vary bubble dynamics and the sharpness of the boundary. Another possibility is that the small percent of noble gas in air can be very important in the behavior of its dielectric constant at high pressure. Furthermore, while small admixtures of noble gas will not significantly alter the zero-frequency refractive index, from the Casimir point of view the behaviour of the refractive index over the entire frequency range up to the cutoff is important. It is also true that magnetic fields are naturally a strong perturbation to the Casimir effect. The presence of an external magnetic field can change the production of particles from the vacuum, in particular it will compete with the time varying external field represented by the changing dielectric constant. If the main source of SL is a dynamical Casimir effect then the phenomenon can be strongly inhibited by a strong enough static magnetic field. On the other hand, the temperature of water can instead affect the dynamics of the bubble boundary by influencing the stability of the bubble, changing either the solubility of air in water or the surface tension of the latter.

In this paper we shall concentrate on changes in the QED vacuum state as a candidate explanation for SL, and try to clear up considerable confusion as to what the Casimir effect model does and does not predict. It is important to realize that the Casimir effect in this experimental situation is big, that it has the right energy budget to drive SL, and that any purported non-Casimir explanation for SL will have to find a way to hide the effects of the Casimir energy so as to make it unobservable.

II. QUANTUM-ELECTRODYNAMIC MODELS OF SL

A. Quasi-static Casimir models: Schwinger's approach

The idea of a “Casimir route” to SL is due to Schwinger who several years ago wrote a series of papers [2–8] regarding the so-called dynamical Casimir effect. Considerable confusion has been caused by Schwinger's choice of the phrase “dynamical Casimir effect” to describe his model. In fact, the original model is not dynamical and is at best quasi-static as the heart of the model lies in comparing two static Casimir energy calculations: that for an expanded bubble with that for a collapsed bubble. One key issue in Schwinger's model is thus simply that of calculating Casimir energies for dielectric spheres—there is already considerable disagreement on this issue. A second and in some ways more critical question is the extent to which this difference in Casimir energies may be converted to real photons during the collapse of the bubble—it is this issue that we shall address in this paper. We estimate the spectrum of the emitted photons by calculating an appropriate Bogolubov coefficient relating the two states of the QED vacuum. In contrast the model of Eberlein [9–11] (more fully discussed below) is truly dynamical but uses a radically different physical approximation — the adiabatic approximation. The two models should not be confused.

In a series of papers [2–8] Schwinger showed that the dominant bulk contribution to the Casimir energy of a bubble (of dielectric constant ϵ_{inside}) in a dielectric background (of dielectric constant $\epsilon_{outside}$) is

$$\begin{aligned} E_{cavity} &= +2 \frac{4\pi}{3} R^3 \int_0^K \frac{4\pi k^2 dk}{(2\pi)^3} \frac{1}{2} \hbar c k \left(\frac{1}{\sqrt{\epsilon_{inside}}} - \frac{1}{\sqrt{\epsilon_{outside}}} \right) + \dots \\ &= +\frac{1}{6\pi} \hbar c R^3 K^4 \left(\frac{1}{\sqrt{\epsilon_{inside}}} - \frac{1}{\sqrt{\epsilon_{outside}}} \right) + \dots \end{aligned} \quad (1)$$

There are additional sub-dominant finite volume effects [12–14]. The quantity K is a high-wavenumber cutoff that characterizes the wavenumber at which the dielectric constants drop to their vacuum values. This result can also be rephrased in the clearer and more general form as [12–14]:

$$E_{cavity} = +2V \int \frac{d^3 \vec{k}}{(2\pi)^3} \frac{1}{2} \hbar [\omega_{inside}(k) - \omega_{outside}(k)] + \dots \quad (2)$$

where it is evident that the Casimir energy can be interpreted as a difference in zero point energies due to the different dispersion relations inside and outside the bubble.

The three main points of strength of models based on zero point fluctuations (e.g. Schwinger's model and its variants, the Eberlein model and its variants) are:

1) The vacuum production of photon pairs allows for the very short timescales that one requires to fit data. Typically one expects these timescales to be of the order of the time that the zero point modes of the EM field takes to be correlated on the bubble scale. (Roughly the light-crossing time for the bubble.) For a bubble of radius 0.5 microns this time scale is about 1.6 femtoseconds, 10^{-3} ps, which is certainly sufficiently rapid to be compatible with observed flash duration. (Though there have been claims that flash duration is less than 10^{-1} ps, recent experiments place flash duration in the range 50 – 250 ps [15,16].)

2) One does *not* need to achieve "real" temperatures of thousands of Kelvin inside the bubble. Quasi-thermal behaviour is generated in quantum vacuum models by the squeezed nature of the two photon states created [10], and the "temperature" parameter is a measure of the squeezing, not a measure of any real physical temperature. (Of course, one should remember that the experimental data merely indicates an approximately power-law spectrum [$N(\omega) \propto \omega^\alpha$] with some sort of cutoff in the ultraviolet, and with an exponent that depends on the gasses entrained in the bubble; the much quoted "temperature" of the SL radiation is merely an indication of the scale of this cutoff.)

3) There is no actual production of far ultraviolet photons (because the refractive index goes to unity in the far ultraviolet) so one does not expect dissociation effects in water that other models imply. Models based on the quantum vacuum automatically provide a cutoff in the far ultraviolet from the behaviour of the refractive index — this observation going back to Schwinger's first papers on the subject.

In contrast, Milton [17], and Milton and Ng [18,19] strongly criticize Schwinger's result claiming that actually the Casimir energy contains at best a surface term, the bulk term simply being discarded via a (physically dubious) renormalization argument. In their most recent paper [19] they discard even the surface term and now claim that the Casimir energy for a dielectric bubble is of order $E \approx \hbar c/R$. These points have been discussed extensively in [12–14] where it is emphasized that one has to compare two different geometrical configurations, and different quantum states, of the same spacetime regions. This point of view is also in agreement with the bag model results of Candelas [20]. It is easy to see that in the bag model one finds a bulk contribution that happens to be zero only because of the particular condition that $\epsilon\mu = 1$ everywhere. This condition ensures the constancy of the speed of light (and so the invariance of the dispersion relation) on all space while allowing the dielectric constant to be less than one outside the vacuum bag (as the model for quark confinement requires). In a situation like Schwinger's model for SL one has to subtract from the zero point energy (ZPE) for a vacuum bubble in water the ZPE for water filling all space. It is clear that in this case the bulk term is physical and *must* be taken into account. Surface terms are also present, and eventually other higher order correction terms, but they prove to not be dominant for sufficiently large cavities [14].

The calculations of Brevik *et al* [21] and Nesterenko and Pirozhenko [22] also fail to retain the known bulk volume term. In this case the subtlety in the calculation arises from neglecting the continuum part of the spectrum. They consider a dielectric sphere in an infinite dielectric background and sum *only* over the discrete part of the spectrum to calculate their Casimir "energy". When the continuum modes are reintroduced the proper volume dependence is recovered. Their conclusions regarding the relevance of the Casimir effect to SL are then incorrect: by completely discarding the volume (and indeed surface) contribution they are left with a Casimir "energy" that can be simply estimated by dimensional analysis to be of order $\hbar c/R$ and is strictly proportional to the inverse radius of the bubble. This is certainly a very small quantity insufficient to drive SL (and the wrong sign to boot) but this is also not the correct physical quantity to calculate. For a careful discussion of the correct identification of the physically relevant Casimir energy see [12–14].

As a last comment about this discussion regarding the presence of the bulk contribution we want to stress a recent comment by Barber *et al.* [1]. They claimed that in Schwinger's formulation the main production of photons may be expected when the the rate of change of the volume is maximum, which they assert is experimentally found to occur near the maximum radius. In contrast the emission of light is experimentally found to occur near the point of minimum radius, where they assert that rate of change of area would be maximum. *All else being equal*, this would seem to indicate a surface dependence and might be interpreted as a true weakness of the dynamical Casimir explanation of SL. In fact we shall show that the situation is considerably more complex than might naively be thought.

B. Eberlein's dynamical model for SL

The quantum vacuum based approach to SL was taken in a new direction by the work of Eberlein [9–11] who managed to formulate the first truly dynamical model of photon pair creation by a moving dielectric boundary. The basic mechanism in Eberlein's approach is a dynamical Casimir effect: Photons are produced due to an *adiabatic*

change of the refractive index in the portion of space between the minimum and the maximal bubble radius (a related discussion for time-varying refractive index can be found in [23]). This physical framework is actually implemented via a boundary between two dielectric media which accelerates with respect to the rest frame of the quantum vacuum state. The non-adiabatic change in the zero-point modes of the fields reflects in a non-zero radiation flux.

It is important to realize that this is a second-order effect. Schwinger's mechanism is posited on the direct conversion of zero point fluctuations in the expanded bubble vacuum state into real photons plus zero point fluctuations in the collapsed bubble vacuum state. Eberlein's mechanism is a more subtle (and much weaker) effect involving the response of the atoms in the dielectric medium to acceleration through the zero-point fluctuations. The two mechanisms are quite distinct and considerable confusion has been engendered by conflating the two mechanisms. Criticisms of the Eberlein mechanism do not necessarily apply to the Schwinger mechanism, and vice versa.

In the Eberlein analysis the motion of the bubble boundary is taken into account by introducing a velocity-dependent perturbation to the usual EM Hamiltonian:

$$H_\epsilon = \frac{1}{2} \int d^3r \left(\frac{\mathbf{D}^2}{\epsilon} + \mathbf{B}^2 \right), \quad (3)$$

$$\Delta H = \beta \int d^3r \frac{\epsilon - 1}{\epsilon} (\mathbf{D} \wedge \mathbf{B}) \cdot \hat{\mathbf{r}}. \quad (4)$$

This is an approximate low-velocity result coming from a power series expansion in the speed of the bubble wall $\beta = \dot{R}/c$. (The bubble wall is known to collapse with supersonic velocity, values of Mach 4 to Mach 10 are often quoted, but this is still completely non-relativistic with $\beta \approx 10^{-5}$. Unfortunately, when the Eberlein formalism is used to model the observed quantity of radiation from each SL flash the implied bubble wall velocities are superluminal, indicating that one has moved outside the region of validity of the approximation scheme.)

The Eberlein approach consists of a novel mixture of the standard adiabatic approximation with perturbation theory. In principle, the adiabatic approximation requires the knowledge of the complete set of eigenfunctions of the Hamiltonian for any allowed value of the parameter. In the present case only the eigenfunctions of part of the Hamiltonian, namely those of H_ϵ , are known. (And these eigenfunctions are known explicitly only in the adiabatic approximation where ϵ is treated as time-independent.) The calculation consists of initially invoking the standard application of the adiabatic approximation to the full Hamiltonian, then formally calculating the transition coefficients for the vacuum to two photon transition to first order in β , and finally in explicitly calculating the radiated energy and spectral density. In this last step Eberlein used an approximation valid only in the limit $kR > 1$ which means in the limit of photon wavelengths smaller than the bubble radius. This implies that the calculation will completely miss any resonances that are present.

Eberlein's final result for the energy radiated over one acoustic cycle is:

$$\mathcal{W} = 1.16 \frac{(n^2 - 1)^2}{n^2} \frac{1}{480\pi} \left[\frac{\hbar}{c^3} \right] \int_0^T d\tau \frac{\partial^5 R^2(\tau)}{\partial \tau^5} R(\tau) \beta(\tau). \quad (5)$$

(Eberlein approximates $n_{inside} \approx n_{air} \approx 1$ and sets $n_{outside} = n_{water} \rightarrow n$. The 1.16 is the result of an integration that has to be estimated numerically. The precise nature of the semi-analytic approximations made as prelude to performing the numerical integration are far from clear.)

One of the interesting consequences of this result is that the dissipative force acting on the moving dielectric interface can be seen to behave like $R^2 \beta^{(4)}(t)$, plus terms with lower derivatives of β . This dependence tallies with results of calculations for frictional forces on moving perfect mirrors; the dissipative part of the radiation pressure on a moving dielectric or mirror is proportional to the fourth derivative of the velocity.

By a double integration by parts the above can be re-cast as

$$\mathcal{W} = 1.16 \frac{(n^2 - 1)^2}{n^2} \frac{1}{960\pi} \left[\frac{\hbar}{c^4} \right] \int_0^T d\tau \left(\frac{\partial^3 R^2(\tau)}{\partial \tau^3} \right)^2. \quad (6)$$

Then the energy radiated is also seen to be proportional to

$$\int_0^T (\dot{R})^2 (\ddot{R})^2 + \dots \quad (7)$$

explicitly showing that the acceleration of the interface (\ddot{R}) and the strength of the perturbation (\dot{R}) both contribute to the radiated energy.

In this mechanism the massive burst of photons is produced at and near the turn-around at the minimum radius of the bubble. There the velocity rapidly changes sign, from collapse to re-expansion. This means that the acceleration is peaked at this moment, and so are higher derivatives of the velocity.

The main points of strength of the Eberlein model are the same as previously listed for the Schwinger model. However, Eberlein's model exhibits significant weaknesses (which do not apply to the Schwinger model):

1) The calculation is based on an adiabatic approximation which does not seem consistent with results. The adiabatic approximation would seem to be justified in the SL case by the fact that the frequency Ω of the driving sound is of the order of tens of kHz, while that of the emitted light is of the order of 10^{16} Hz. But it is questionable if in Eberlein's model this is the right condition to impose. In fact Eberlein considers just one cycle of contraction and re-expansion of the bubble, so it is unclear what is the typical frequency to take into account for a test of the applicability of the adiabatic approximation.

Actually in order to fit the experimental values the model requires, as an external input, the bubble radius time dependence. This is expressed as a function of a parameter γ which describes the time scale of the collapse and re-expansion process. In order to fit the experimental values for \mathcal{W} one has to fix $\gamma \approx 10\text{fs}$. This is far too short a time to be compatible with experimental data. Although one may claim that this number can ultimately be modified by the eventual presence of resonances it would seem reasonable to take this ten femtosecond figure as a first self-consistent approximation for the characteristic timescale of the driving system (the pulsating bubble). Unfortunately, the characteristic timescale of the collapsing bubble then comes out to be of the same order of the characteristic period of the emitted photons. This shows that attempts at bootstrapping the calculation into self-consistency instead bring it to a regime where the adiabatic approximation underlying the scheme cannot be trusted.

2) The Eberlein calculation cannot deal with any resonances that may be present. Eberlein does consider resonances to be a possible important correction to her model, but she is considering "classical" resonances (scale of the cavity of the same order of the wavelength of the photons) instead of what we feel is the more interesting possibility of parametric resonances.

3) A very recent calculation which should give qualitatively the same results as the Eberlein model leads to strangely different formulae, and the discrepancy is not easy to understand. Schützhold, Plunien, and Soff [24] adopt a slightly different decomposition into unperturbed and perturbing Hamiltonians by taking

$$H_0 = \frac{1}{2} \int d^3r \left(\frac{\mathbf{D}^2}{\epsilon_0} + \mathbf{B}^2 \right), \quad (8)$$

$$\Delta H = \int d^3r \left(-\frac{1}{2} \frac{\epsilon - \epsilon_0}{\epsilon \epsilon_0} \mathbf{D}^2 + \beta \frac{\epsilon - \epsilon_0}{\epsilon} (\mathbf{D} \wedge \mathbf{B}) \cdot \hat{\mathbf{r}} \right), \quad (9)$$

Their result for the total energy emitted per cycle is given analytically by

$$\mathcal{W} = \frac{n^2(n^2 - 1)^2}{1890\pi} \left[\frac{\hbar}{c^6} \right] \int_0^T d\tau \left(\frac{\partial^4 R^3(\tau)}{\partial \tau^4} \right)^2. \quad (10)$$

The key differences are that this formula is analytic (rather than numerical) and involves fourth derivatives of the volume of the bubble (rather than third derivatives of the surface area). This might best be interpreted as suggesting that there are still some theoretical uncertainties regarding application of, and calculation in, the Eberlein model.

Putting these models aside, and before proposing new routes for developing further research in SL, we shall give below a more detailed discussion of some important points of Schwinger's model which seemed crucial in order to understand the possibility of a vacuum explanation of SL.

III. BOGOLUBOV COEFFICIENTS

As a first approach to the problem we decided to study in detail the basic mechanism of particle creation and to test the consistency of the Casimir energy proposals previously described. With this aim in mind we studied a single pulsation of the bubble. At this stage of development, we are not concerned with the dynamics of the bubble surface. In analogy with the subtraction procedure of the static calculations of Schwinger [2–8] or of Carlson et al. [12–14] we shall consider two different configurations of space. An "in" configuration with a bubble of dielectric constant ϵ_{inside} (typically vacuum) in a medium of dielectric constant $\epsilon_{outside}$, and an "out" one in which one has just the latter medium (dielectric constant $\epsilon_{outside}$) filling all space. (Strictly speaking we should compare a large bubble with a small bubble. We are approximating the small bubble by zero volume on the grounds that the small bubble that is relevant to SL is at least a million times smaller than the large bubble at the expansion maximum.) These two configurations will correspond to two different bases for the quantization of the field. (For the sake of simplicity we

take, as Schwinger did, only the electric part of QED, reducing the problem to a scalar electrodynamics). The two bases will be related by Bogolubov coefficients in the usual way. Once we determine these coefficients we easily get the number of created particles per mode and from this the spectrum. (This tacitly makes the “sudden approximation”: Changes in the refractive index are assumed to be non-adiabatic, see [25] and the appendix for more discussion.) We shall also make a consistency check by a direct confrontation between the change in Casimir energy and the direct sum, $E = \sum_k \omega_k n_k$ of the energies of the created photons. The former energy (the total energy of the particles that can be produced by the collapse) must necessarily equal the Casimir energy of the bubble in the “in” state since in the current simplified model there is no external source of energy (like the driving sound in the true dynamical effect). For this reason we expect to be able to give a definitive answer on the nature (dependence on the bubble radius and on the cut-off) of the static Casimir energy. Of course it is evident that such a model cannot be considered a fully satisfactory model for SL. In fact it is just a semi-static approach which completely misses the dependence on time (no dynamics) and moreover by considering just one cycle implies impossibility of testing for the possible presence of parametric resonances. We thus consider it as a toy model in which some basic features of the Casimir approach to SL are described; a test of the effective nature and quantity of the particles produced by a collapsing dielectric bubble in the sudden approximation.

A. Formal calculation

Let us consider the equations of the electric fields (Schwinger framework) in spherical coordinates and with a time independent dielectric constant (we temporarily set $c = 1$ for ease of notation, and shall reintroduce appropriate factors of the speed of light when needed for clarity)

$$\epsilon \partial_0(\partial_0 E) - \nabla^2 E = 0. \quad (11)$$

We look for solutions of the form

$$E = \Phi(r, t) Y_{lm}(\Omega) \frac{1}{r}. \quad (12)$$

Then one finds

$$\epsilon(\partial_0^2 \Phi) - (\partial_r^2 \Phi) + \frac{1}{r^2} l(l+1) \Phi = 0. \quad (13)$$

For both the “in” and “out” solution the field equation in r is given by:

$$\epsilon \partial_0^2 \Phi - \partial_r^2 \Phi + \frac{1}{r^2} l(l+1) \Phi = 0. \quad (14)$$

In both asymptotic regimes (past and future) one has a static situation (a bubble in the dielectric, or just the dielectric) so one can in this limit factorize the time and radius dependence of the modes: $\Phi(r, t) = e^{i\omega t} f(r)$. One gets

$$f'' + \left(\epsilon \omega^2 - \frac{1}{r^2} l(l+1) \right) f = 0. \quad (15)$$

This is a well known differential equation. To handle it more easily in a standard way we can cast it as an eigenvalues problem

$$f'' - \left(\frac{1}{r^2} l(l+1) \right) f = -\lambda^2 f, \quad (16)$$

where $\lambda^2 = \epsilon \omega^2$. With the change of variables $f = r^{1/2} G$ we get

$$G'' + \frac{1}{r} G' + \left(\lambda^2 - \frac{\nu^2}{r^2} \right) G = 0. \quad (17)$$

This is the standard Bessel equation. It admits as solutions the first type Bessel and Neumann functions, $J_\nu(\lambda r)$ and $N_\nu(\lambda r)$, with $\nu = l + 1/2$. Remember that for those solutions which have to be well-defined at the origin, $r = 0$, regularity implies the absence of the Neumann functions. For the “in” basis we have to take into account that the dielectric constant changes at the bubble radius (R). In fact we have

$$\epsilon = \begin{cases} \epsilon_{inside} = n_{gas}^2 & = \text{dielectric constant of air-gas mixture} & \text{if } r \leq R, \\ \epsilon_{outside} = n_{liquid}^2 & = \text{dielectric constant of ambient liquid (typically water)} & \text{if } r > R. \end{cases} \quad (18)$$

Typically one simplifies calculations by using the fact that the dielectric constant of air is approximately equal 1 at standard temperature and pressure (STP), and then dealing only with the dielectric constant of water ($n_{liquid} = \sqrt{\epsilon_{outside}} \approx 1.3$). We wish to avoid this temptation on the grounds that the sonoluminescent flash is known to occur within 500 picoseconds of the bubble achieving minimum radius. Under these conditions the gasses trapped in the bubble are close to the absolute maximum density implied by the hard core repulsion incorporated into the van der Waals equation of state. Gas densities are approximately one million times atmospheric and conditions are nowhere near STP. For this reason we shall explicitly keep track of n_{gas} and n_{liquid} in the formalism we develop. Defining ω_{in} and ω_{out} respectively the in and out frequencies one has

$$G_\nu^{in}(n_{gas}, n_{liquid}, \omega_{in}, r) = \begin{cases} A_\nu J_\nu(n_{gas} \omega_{in} r) & \text{if } r \leq R, \\ B_\nu J_\nu(n_{liquid} \omega_{in} r) + C_\nu N_\nu(n_{liquid} \omega_{in} r) & \text{if } r > R. \end{cases} \quad (19)$$

The A_ν , B_ν , and C_ν coefficients are determined by matching conditions in R

$$\begin{aligned} A_\nu J_\nu(n_{gas} \omega_{in} R) &= B_\nu J_\nu(n_{liquid} \omega_{in} R) + C_\nu N_\nu(n_{liquid} \omega_{in} R), \\ A_\nu J_\nu'(n_{gas} \omega_{in} R) &= B_\nu J_\nu'(n_{liquid} \omega_{in} R) + C_\nu N_\nu'(n_{liquid} \omega_{in} R). \end{aligned} \quad (20)$$

The “out” basis is easily obtained solving the same equation but for a space filled with a homogeneous dielectric,

$$G_\nu^{out}(n_{liquid}, \omega_{out}, r) = J_\nu(n_{liquid} \omega_{out} r). \quad (21)$$

To check that the “out” basis is properly normalized we use the scalar product, defined as usual by

$$(\phi_1, \phi_2) = -i \int_{\Sigma} \phi_1 \overleftrightarrow{\partial}_0 \phi_2^* d^3x. \quad (22)$$

In our case we shall deal with the scalar product of a eigenfunction with itself, one expects to obtain a normalization condition which can be written as

$$((\Phi_{out}^i)^*, (\Phi_{out}^j)^*) = \delta^{ij}. \quad (23)$$

Inserting the explicit form of the Φ functions we get

$$((\Phi_{out}^i)^*, (\Phi_{out}^j)^*) = (\lambda + \lambda') \int_0^\infty r dr J_\nu(\lambda r) J_\nu(\lambda' r) e^{i(\lambda - \lambda')} \quad (24)$$

$$= (\lambda + \lambda') \frac{\delta(\lambda - \lambda')}{\lambda} e^{i(\lambda - \lambda')}, \quad (25)$$

where we have used the Hankel Integral Formula [26]

$$\int_0^\infty r dr J_\nu(\lambda r) J_\nu(\lambda' r) = \delta(\lambda - \lambda')/\lambda. \quad (26)$$

The Bogolubov coefficients are *defined* as

$$\alpha_{ij} = -(E_i^{out*}, E_j^{in*}), \quad (27)$$

$$\beta_{ij} = (E_i^{out}, E_j^{in*}). \quad (28)$$

We are mainly interested in the coefficient β , since $|\beta|^2$ is linked to the total number of particles created. By a direct substitution it is easy to find the expression for the Bogolubov coefficients we are interested in:

$$\beta = -i \int_0^\infty \left(\Phi_{out}(r, t) Y_{lm}(\Omega) \frac{1}{r} \right) \overleftrightarrow{\partial}_0 \left(\Phi_{in}(r, t) Y_{l'm'}(\Omega) \frac{1}{r} \right)^* r^2 dr d\Omega, \quad (29)$$

$$= (\omega_{in} - \omega_{out}) e^{i(\omega_{out} + \omega_{in})t} \delta_{ll'} \delta_{mm'} \int_0^\infty G_l^{out}(n_{liquid}, \omega_{out}, r) G_{l'}^{in}(n_{gas}, n_{liquid}, \omega_{in}, r) r dr. \quad (30)$$

To compute the integral one needs some ingenuity, let us write the equations of motion for two different values of the eigenvalues, λ and μ .

$$G_\lambda'' + \frac{1}{r} G_\lambda' + \left(\lambda^2 - \frac{1}{r^2} (l + \frac{1}{2})^2 \right) G_\lambda = 0, \quad (31)$$

$$G_\mu'' + \frac{1}{r} G_\mu' + \left(\mu^2 - \frac{1}{r^2} (l + \frac{1}{2})^2 \right) G_\mu = 0. \quad (32)$$

If we multiply the first by G_μ and the second by G_λ we get

$$G_\lambda'' G_\mu + \frac{1}{r} G_\lambda' G_\mu + \left(\lambda^2 - \frac{1}{r^2} (l + \frac{1}{2})^2 \right) G_\lambda G_\mu = 0, \quad (33)$$

$$G_\mu'' G_\lambda + \frac{1}{r} G_\mu' G_\lambda + \left(\mu^2 - \frac{1}{r^2} (l + \frac{1}{2})^2 \right) G_\mu G_\lambda = 0. \quad (34)$$

Subtracting the second from the first we then obtain

$$(G_\lambda'' G_\mu - G_\mu'' G_\lambda) + \frac{1}{r} (G_\lambda' G_\mu - G_\mu' G_\lambda) + (\lambda^2 - \mu^2) G_\lambda G_\mu = 0. \quad (35)$$

The second term on the left hand side is a pseudo-Wronskian determinant

$$W_{\lambda\mu}(r) = G_\lambda'(r) G_\mu(r) - G_\mu'(r) G_\lambda(r), \quad (36)$$

and the first term is its total derivative $dW_{\lambda\mu}/dr$. It's a pseudo-Wronskian, not a true Wronskian, since the two functions G_λ and G_μ correspond to different eigenvalues and so solve different differential equations. The derivatives are all with respect to the variable r . Using this definition we can cast the integral over r of the product of two given solutions into a simple form. Generically:

$$(\mu^2 - \lambda^2) \int_a^b r dr G_\lambda G_\mu = \int_a^b r dr dW_{\lambda\mu} + \int_a^b dr W_{\lambda\mu}. \quad (37)$$

That is

$$\int_a^b r dr G_\lambda G_\mu = \frac{1}{(\mu^2 - \lambda^2)} W_{\lambda\mu} r \Big|_a^b - \int_a^b dr W_{\lambda\mu} + \int_a^b dr W_{\lambda\mu}. \quad (38)$$

So the final result is

$$\int_a^b r dr G_\lambda G_\mu = \frac{1}{(\mu^2 - \lambda^2)} (W_{\lambda\mu} r) \Big|_a^b. \quad (39)$$

This expression can be applied in our specific case Eq. (30), we obtain:

$$\int_0^\infty r dr G_\nu^{out}(n_{liquid}, \omega, r) G_\nu^{in}(n_{gas}, n_{liquid}, \omega, r) \quad (40)$$

$$= \int_0^R r dr G_\nu^{out}(n_{liquid} \omega_{out} r) G_\nu^{in}(n_{gas} \omega_{in} r) + \int_R^\infty r dr G_\nu^{out}(n_{liquid} \omega_{out} r) G_\nu^{in}(n_{liquid} \omega_{in} r) \quad (41)$$

$$= \frac{\{rW[G_\nu^{out}(n_{liquid} \omega_{out} r), G_\nu^{in}(n_{gas} \omega_{in} r)]\}_0^R}{(n_{liquid} \omega_{out})^2 - (n_{gas} \omega_{in})^2} + \frac{\{rW[G_\nu^{out}(n_{liquid} \omega_{out} r), G_\nu^{in}(n_{liquid} \omega_{in} r)]\}_0^\infty}{(n_{liquid} \omega_{out})^2 - (n_{liquid} \omega_{in})^2} \quad (42)$$

$$= R \left[\frac{W[G_\nu^{out}(n_{liquid} \omega_{out} r), G_\nu^{in}(n_{gas} \omega_{in} r)]_{R_-}}{(n_{liquid} \omega_{out})^2 - (n_{gas} \omega_{in})^2} - \frac{W[G_\nu^{out}(n_{liquid} \omega_{out} r), G_\nu^{in}(n_{liquid} \omega_{in} r)]_{R_+}}{(n_{liquid} \omega_{out})^2 - (n_{liquid} \omega_{in})^2} \right], \quad (43)$$

where we have used the fact that the above forms are well behaved (and equal to 0) for $r = 0$, and $r = \infty$ by construction. (Here and henceforth we shall automatically give the same l value to the “in” and “out” solutions by using the fact that Eq. (30) contains a Kronecker delta in l and l' .)

Finally the two pseudo-Wronskians so found can be shown to be equal (by the junction condition (20)). In fact one can easily check that:

$$A_\nu W[J_\nu(n_{liquid} \omega_{out} r), J_\nu(n_{gas} \omega_{in} r)]_R = B_\nu W[J_\nu(n_{liquid} \omega_{out} r), J_\nu(n_{gas} \omega_{in} r)]_R + C_\nu W[J_\nu(n_{liquid} \omega_{out} r), N_\nu(n_{gas} \omega_{in} r)]_R. \quad (44)$$

This equality allows to rewrite integral in Eq. (30) in a more compact form

$$\int_0^\infty r \ dr G_\nu^{out}(n_{liquid}, \omega, r) G_\nu^{in}(n_{gas}, n_{liquid}, \omega, r) \quad (45)$$

$$= A_\nu \left[\frac{1}{(n_{liquid} \omega_{out})^2 - (n_{gas} \omega_{in})^2} - \frac{1}{(n_{liquid} \omega_{out})^2 - (n_{liquid} \omega_{in})^2} \right] W[J_\nu(n_{liquid} \omega_{out} r), J_\nu(n_{gas} \omega_{in} r)]_R \quad (46)$$

$$= - \left(\frac{n_{liquid}^2 - n_{gas}^2}{n_{liquid}^2} \right) \frac{A_\nu R \omega_{in}^2}{[\omega_{out}^2 - \omega_{in}^2]} \frac{W[J_\nu(n_{liquid} \omega_{out} r), J_\nu(n_{gas} \omega_{in} r)]_R}{[(n_{liquid} \omega_{out})^2 - (n_{gas} \omega_{in})^2]}. \quad (47)$$

Inserting this expression into Eq. (30) we get

$$\beta = \left(\frac{n_{liquid}^2 - n_{gas}^2}{n_{liquid}^2} \right) \delta_{ll'} \delta_{mm'} \frac{(\omega_{out} - \omega_{in})}{\omega_{out}^2 - \omega_{in}^2} R A_\nu \frac{\omega_{in}^2 W[J_\nu(n_{liquid} \omega_{out} r), J_\nu(n_{gas} \omega_{in} r)]_R}{[(n_{liquid} \omega_{out})^2 - (n_{gas} \omega_{in})^2]} e^{i(\omega_{out} + \omega_{in})t}. \quad (48)$$

We are mainly interested in the square of this coefficient summed over l and m . It is in fact this quantity that is linked to the spectrum of the “out” particles present in the “in” vacuum, and it is this quantity that is related to the total energy emitted. Including all appropriate dimensional factors (c, \hbar) we have

$$\frac{dN(\omega_{out})}{d\omega_{out}} = \left(\int |\beta(\omega_{in}, \omega_{out})|^2 d\omega_{in} \right), \quad (49)$$

and

$$E = \hbar \int \frac{dN(\omega_{out})}{d\omega_{out}} \omega_{out} d\omega_{out}. \quad (50)$$

Hence we shall deal with the computation of:

$$|\beta(\omega_{in}, \omega_{out})|^2 = \sum_{lm} \sum_{l'm'} [\beta_{lm, l'm'}(\omega_{in}, \omega_{out})]^2 \quad (51)$$

$$= \left(\frac{n_{liquid}^2 - n_{gas}^2}{n_{liquid}^2} \right)^2 \left(\frac{\omega_{in}^2 R}{\omega_{out} + \omega_{in}} \right)^2 \sum_{l=1}^{\infty} (2l+1) |A_\nu|^2 \left[\frac{W[J_\nu(n_{liquid} \omega_{out} r/c), J_\nu(n_{gas} \omega_{in} r/c)]_R}{(n_{liquid} \omega_{out})^2 - (n_{gas} \omega_{in})^2} \right]^2. \quad (52)$$

This expression is too complex to allow an analytical resolution of the problem. Nevertheless we shall show that the terms appearing in it can be suitably approximated in such a way as to obtain a computable form that shall give us some information about the main predictions of this model. We shall first look at the large volume limit, which will allow us to compare this result to Schwinger’s calculation, and then develop some numerical approximations suitable to estimating the predicted spectra for finite volume.

B. Behaviour in the large R limit

It has been clarified at the start of this section that one of the main objectives of this calculation is to shed some light on the nature of the Casimir energy which have to be transformed in photons. In particular we expect that the total energy of the photons calculated from the Bogolubov approach would give the same results of the static Casimir energy calculations such those of Schwinger, and of Carlson *et al.* [5,17,12] since we have excluded, in this semi-static approach, any external force. We shall start by some general considerations.

From Eq. (52) it is easy to check that the general form of the squared Bogolubov coefficient is given by

$$|\beta(x, y)|^2 = \frac{R^2}{c^2} \beta_0^2(x, y), \quad (53)$$

where $\beta_0^2(x, y)$ is a dimensionless quantity and we introduce dimensionless variables $x = n_{liquid} \omega_{out} R/c$ and $y = n_{gas} \omega_{in} R/c$. (The dimensions of β should always be those of time.) The spectrum is then given by

$$\frac{dN(\omega_{out})}{d\omega_{out}} = \frac{R}{c n_{gas}} \left(\int_0^{RK} |\beta_0(x, y)|^2 dy \right), \quad (54)$$

and the energy radiated is

$$E = \frac{\hbar c}{n_{liquid}^2 n_{gas} R} \int_0^\infty dx \int_0^{RK} dy x |\beta_0(x, y)|^2. \quad (55)$$

If R is very large (but finite in order to avoid infra-red divergences) then the “in” and the “out” modes can both be described by ordinary Bessel functions

$$G^{in}(n_{gas}, \omega, r) = J_\nu(n_{gas} \omega_{in} r / c), \quad (56)$$

$$G^{out}(n_{liquid}, \omega, r) = J_\nu(n_{liquid} \omega_{out} r / c). \quad (57)$$

We can now compute the Bogolubov coefficient relating these states

$$\beta_{ij} = (E_i^{out}, E_j^{in*}) \quad (58)$$

$$= \frac{(\omega_{in} - \omega_{out})}{c^2} e^{i(\omega_{out} + \omega_{in})t} \delta_{ll'} \delta_{mm'} \int J_\nu(n_{gas} \omega_{in} r / c) J_\nu(n_{liquid} \omega_{out} r / c) r dr \quad (59)$$

$$= (\omega_{in} - \omega_{out}) e^{i(\omega_{out} + \omega_{in})t} \delta_{ll'} \delta_{mm'} \frac{\delta(n_{gas} \omega_{in} - n_{liquid} \omega_{out})}{n_{gas} \omega_{in}} \quad (60)$$

$$= \left(\frac{1}{n_{gas}} - \frac{1}{n_{liquid}} \right) e^{i\omega_{in}(n_{gas}/n_{liquid}+1)t} \delta_{ll'} \delta_{mm'} \delta(n_{gas} \omega_{in} - n_{liquid} \omega_{out}). \quad (61)$$

This result implies that

$$|\beta(\omega_{in}, \omega_{out})|^2 = \sum_{lm} \sum_{l'm'} |\beta_{lm l'm'}(\omega_{in}, \omega_{out})|^2 \quad (62)$$

$$= \left(\frac{n_{liquid} - n_{gas}}{n_{liquid} n_{gas}} \right)^2 \sum_l (2l+1) \{ \delta(n_{gas} \omega_{in} - n_{liquid} \omega_{out}) \}^2 \quad (63)$$

$$= \left(\frac{n_{liquid} - n_{gas}}{n_{liquid} n_{gas}} \right)^2 \sum_l (2l+1) \delta(0) \delta(n_{gas} \omega_{in} - n_{liquid} \omega_{out}) \quad (64)$$

$$= \left(\frac{n_{liquid} - n_{gas}}{n_{liquid} n_{gas}} \right)^2 \sum_l (2l+1) \frac{R}{2\pi c} \delta(n_{gas} \omega_{in} - n_{liquid} \omega_{out}), \quad (65)$$

where we have invoked the standard scattering theory result

$$\{\delta^3(k)\}^2 = \frac{V}{(2\pi)^3} \delta^3(k), \quad (66)$$

specialized to the fact that we have a 1-dimensional delta function (in frequency, not momentum). The sum over angular momenta (which is formally infinite) can now be estimated as follows

$$\sum_{l=1}^{l_{max}(\omega_{out})} (2l+1) = l_{max}^2(\omega_{out}) - 1 \approx l_{max}^2(\omega_{out}). \quad (67)$$

The angular momentum cutoff is estimated by taking

$$l_{max}(\omega) \approx \frac{(n_{liquid} \hbar \omega_{out} / c) \times R}{\hbar} = n_{liquid} \omega_{out} R / c = x. \quad (68)$$

So in the above we are justified in approximating

$$\sum_l (2l+1) \approx x^2. \quad (69)$$

By changing to the dimensionless variables (x, y) this finally gives

$$|\beta(x, y)|^2 = \left(\frac{n_{liquid} - n_{gas}}{n_{liquid} n_{gas}} \right)^2 \frac{R^2}{2\pi c^2} x^2 \delta(x - y). \quad (70)$$

We can now compute the spectrum and the total energy of the emitted photons

$$\frac{dN(\omega_{out})}{d\omega_{out}} \approx \frac{R}{2\pi c n_{gas}} \left(\frac{n_{liquid} - n_{gas}}{n_{liquid} n_{gas}} \right)^2 \int_0^{RK} x^2 \delta(x - y) dy \quad (71)$$

$$= \frac{R}{2\pi c n_{gas}} \left(\frac{n_{liquid} - n_{gas}}{n_{liquid} n_{gas}} \right)^2 x^2 \Theta(RK - x) \quad (72)$$

$$= \frac{n_{liquid}^2}{n_{gas}} \left(\frac{n_{liquid} - n_{gas}}{n_{liquid} n_{gas}} \right)^2 \frac{R^3 \omega_{out}^2}{2\pi c^3} \Theta(K - n_{liquid} \omega_{out}/c), \quad (73)$$

and

$$E \approx \frac{\hbar c}{2\pi n_{liquid}^2 n_{gas} R} \left(\frac{n_{liquid} - n_{gas}}{n_{liquid} n_{gas}} \right)^2 \int_0^\infty dx \int_0^{RK} x \times x^2 \times \delta(x - y) dy \quad (74)$$

$$= \frac{\hbar c}{2\pi n_{liquid}^2 n_{gas} R} \left(\frac{n_{liquid} - n_{gas}}{n_{liquid} n_{gas}} \right)^2 \int_0^{RK} dx x^3 \quad (75)$$

$$= \frac{\hbar c}{2\pi n_{liquid}^2 n_{gas} R} \left(\frac{n_{liquid} - n_{gas}}{n_{liquid} n_{gas}} \right)^2 \frac{(RK)^4}{4} \quad (76)$$

$$= \frac{1}{8\pi n_{liquid}^2 n_{gas}} \left(\frac{n_{liquid} - n_{gas}}{n_{liquid} n_{gas}} \right)^2 \hbar c K (RK)^3. \quad (77)$$

Hence, feeding our results (70) into Eqs. (54) and (55) for $dN(\omega)/d\omega$ and E , we exactly reproduce the Schwinger and Carlson *et al.* results. We view this as definitive proof that indeed Schwinger was essentially correct; that the main effect for the Casimir energy of a dielectric bubble is a bulk one, and that the change in Casimir energies can be converted into real photons. (With considerably more brute force analysis the same result can also be obtained directly from Eq. (52) by formally taking the $R \rightarrow \infty$ limit and using the asymptotic formulae for the Bessel functions.) For future comparison purposes it is convenient to write the spectrum in dimensionless form as

$$\frac{dN}{dx} \approx \frac{1}{2\pi n_{liquid} n_{gas}} \left(\frac{n_{liquid} - n_{gas}}{n_{liquid} n_{gas}} \right)^2 x^2 \Theta(RK - x). \quad (78)$$

We now turn to the study of the predictions of the model in the case of finite radius. Unfortunately this cannot be done in an analytic way due to the wild behaviour of the pseudo-Wronskian of the Bessel function. Nevertheless some ingenuity and a detailed study of the different parts of the Bogolubov coefficient leads to reasonable approximations that allow a clear description of the spectrum of particle predicted by the model.

C. The A factor

The A_λ , B_μ , and C_μ factors can be obtained by a two step calculation. First one must solve the system (20) by expressing B and C as functions of A . Then one can fix A by requiring $B^2 + C^2 = 1$, a condition which comes from the asymptotic behaviour of the Bessel functions. Following this procedure, and again suppressing factors of c for notational convenience, we get

$$A_\nu = \frac{W[J_\nu(n_{liquid} \omega_{in} r), N_\nu(n_{liquid} \omega_{in} r)]}{\sqrt{W[J_\nu(n_{gas} \omega_{in} r), N_\nu(n_{gas} \omega_{in} r)]^2 + W[J_\nu(n_{liquid} \omega_{in} r), J_\nu(n_{liquid} \omega_{in} r)]^2}} \Big|_R, \quad (79)$$

$$B_\nu = A_\nu \frac{W[J_\nu(n_{gas} \omega_{in} r), N_\nu(n_{liquid} \omega_{in} r)]}{W[J_\nu(n_{liquid} \omega_{in} r), N_\nu(n_{liquid} \omega_{in} r)]} \Big|_R, \quad (80)$$

$$C_\nu = A_\nu \frac{W[J_\nu(n_{liquid} \omega_{in} r), J_\nu(n_{gas} \omega_{in} r)]}{W[J_\nu(n_{liquid} \omega_{in} r), N_\nu(n_{liquid} \omega_{in} r)]} \Big|_R. \quad (81)$$

We are mostly interested in the coefficient A_ν . This can be simplified by using a well known formula (Abramowitz-Stegun, page 360 formula 9.1.16) for the (true) Wronskian of Bessel functions of the first and second kind.

$$W_{true}[J_\nu(z), N_\nu(z)] = \frac{2}{\pi z}. \quad (82)$$

In our case, taking into account that for our pseudo Wronskian the derivatives are with respect to r (not with respect to z), one gets for the numerator of A_ν :

$$W[J_\nu(n_{liquid} \omega_{in} r), N_\nu(n_{liquid} \omega_{in} r)]_R = n_{liquid} \omega_{in} \frac{2}{\pi(n_{liquid} \omega_{in} R)} = \frac{2}{\pi R}. \quad (83)$$

Hence the A_ν can be written as

$$|A_\nu|^2 = \frac{4/(\pi^2 R^2)}{W[J_\nu(n_{gas} \omega_{in} r), N_\nu(n_{liquid} \omega_{in} r)]^2 + W[J_\nu(n_{gas} \omega_{in} r), J_\nu(n_{liquid} \omega_{in} r)]^2}_R. \quad (84)$$

For $\omega \rightarrow \infty$ at l fixed the asymptotic behaviour is

$$|A_\nu|^2 \sim \frac{2n_{gas} n_{liquid}}{n_{gas}^2 + n_{liquid}^2 + (n_{liquid}^2 - n_{gas}^2) \cos(2n_{gas} \omega_{in} - (\nu + 1/2)\pi)}. \quad (85)$$

Numerical plots of $|A_\nu|^2$ show that it is an oscillating function which rapidly reaches this asymptotic form.

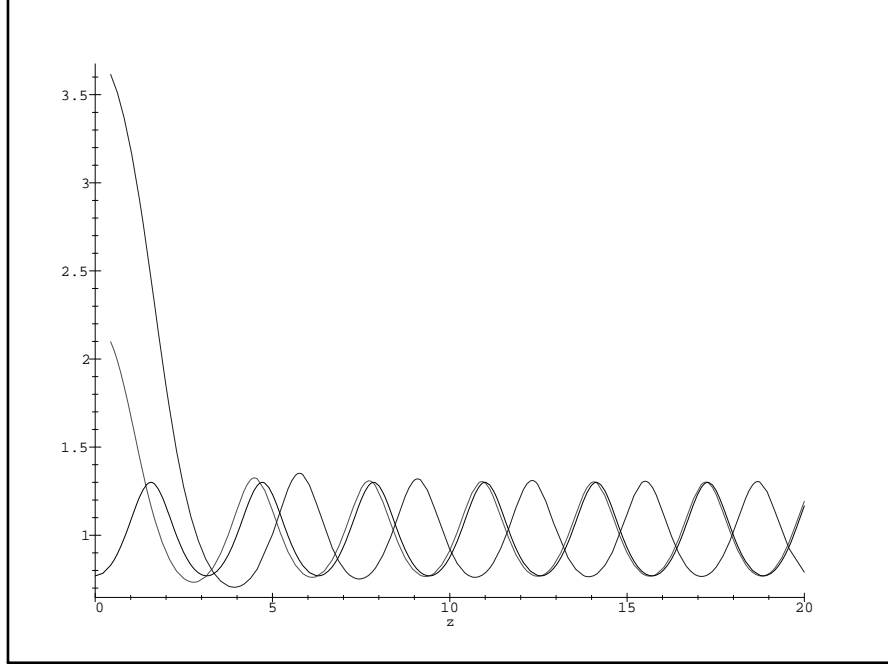


FIG. 1. Plot of $|A_l|^2$ for $\nu = 3/2$ and $\nu = 5/2$. (Here we define $z = \omega R/c$ and put $n_{gas} = 1$, $n_{liquid} = 1.3$.) The function rapidly stabilizes to the asymptotic behavior. The dotted curve shows the behaviour of the asymptotic form for $\nu = 3/2$.

We shall use this approximation to replace the A_ν factor with its mean value for large arguments:

$$|A_\nu|^2 \approx \frac{1}{2\pi} \int_0^{2\pi} dz \frac{2n_{gas} n_{liquid}}{n_{gas}^2 + n_{liquid}^2 + (n_{liquid}^2 - n_{gas}^2) \cos(z)} = 1. \quad (86)$$

That this approximation is adequate may be checked *a posteriori* by seeing that the Bogoliubov coefficients are not noticeably affected.

D. The Pseudo-Wronskian

Use the simplified notation in which $x = n_{liquid} \omega_{out} R/c$, $y = n_{gas} \omega_{in} R/c$. In these dimensionless quantities, after including the approximation Eq. (86), and making explicit the dependence on R and c , Eq. (52) takes the form:

$$|\beta(x, y)|^2 = \frac{R^2}{c^2} \frac{(n_{liquid}^2 - n_{gas}^2)^2}{n_{liquid}^2 n_{gas}^2} \left(\frac{y^2}{n_{gas} x + n_{liquid} y} \right)^2 F(x, y). \quad (87)$$

Here $F(x, y)$ is shorthand for the function

$$F(x, y) = \sum_{l=1}^{\infty} (2l+1) \frac{\left| \begin{array}{cc} J_{\nu}(x) & J_{\nu}(y) \\ x J'_{\nu}(x) & y J'_{\nu}(y) \end{array} \right|^2}{(x^2 - y^2)^2}, \quad (88)$$

where in this equation the primes now signify derivatives with respect to the full arguments (x or y).

In order to proceed in our analysis we need now to perform the summation over angular momentum. Although the infinite sum is analytically intractable, there are two reasonable arguments (one physical and one mathematical) both leading to the conclusion that suitable truncations of this sum will be enough for our purposes.

The first argument is a physical one and it is based on the maximum amount of angular momentum that an outgoing photon may have. Basically, if one supposes the photons to be produced inside or at most on the surface of the bubble, the upper limit for the angular momentum will be the product of the bubble radius times the maximal “out” momentum. Then one gets:

$$l_{max}(K) = \frac{R(\hbar K)}{\hbar} = RK. \quad (89)$$

For SL K is of order $1/(200\text{nm})$. Deciding the appropriate value of R is more tricky. Since the SL flash occurs at or near the moment of minimum radius one might wish to use $R_{min} \approx 500\text{nm}$ in which case $l_{max}(K) \approx 2.5$. Certainly for this choice of R keeping the first ten or so terms will be sufficient. More conservatively, one might wish to choose R to be of order $R_{ambient} \approx 4.5\mu\text{m}$ in which case $l_{max}(K) \approx 25$. Keeping this number of terms in the series is already very unwieldy. Finally, in Schwinger’s original version of the model it is the change in Casimir energy during the collapse all the way from maximum radius that is relevant, so perhaps one should use $R_{max} \approx 45\mu\text{m}$. In this case $l_{max}(K) \approx 250$, and explicit summation of the series is prohibitively difficult. To handle these problems we develop a semi-analytic approximation to the sum which is sufficient for making numerical estimates of the spectrum.

This argument can be bolstered by considering the large order expansion ($\nu \rightarrow \infty$ at fixed x) of the Bessel functions. In this limit one gets [27]:

$$J_{\nu}(x) \sim \frac{1}{\sqrt{2\pi\nu}} \left(\frac{ex}{2\nu} \right)^{\nu} \quad (90)$$

This can be used to obtain the asymptotic form of the pseudo-Wronskian appearing in Eq. (88).

$$\tilde{W}_{\nu}(x, y) \equiv \left| \begin{array}{cc} J_{\nu}(x) & J_{\nu}(y) \\ x J'_{\nu}(x) & y J'_{\nu}(y) \end{array} \right| \quad (91)$$

$$= - \left| \begin{array}{cc} J_{\nu}(x) & J_{\nu}(y) \\ x J_{\nu+1}(x) & y J_{\nu+1}(y) \end{array} \right| \quad (92)$$

$$\sim \frac{(x^2 - y^2)}{2\pi(\nu)^{1/2}(\nu+1)^{3/2}} \left(\frac{xy}{\nu(\nu+1)} \right)^{\nu} \left(\frac{e}{2} \right)^{2\nu+1}. \quad (93)$$

where we have used the standard recursion relation for the Bessel functions $J'_{\nu}(z) = \nu J_{\nu}(z) - z J_{\nu+1}(z)$. This indicates that the sum over ν is convergent: the terms for which $(xy/\nu^2) \leq 1$ are suppressed. Since, depending on one’s views as to the appropriate value of R , x and y are at most of order 2.5, 25, or 250 we deduce that the maximal contribution to the sum comes from a limited number of terms.

Analytically, it is easy to see that the function $F(x, y)$ is finite along the diagonal and goes smoothly to zero for $x, y \rightarrow 0$. To proceed to an actual computation of the predicted spectrum we need to develop an semi-analytic approximate form for this function by considering separately the behaviour along the diagonal $x - y = 0$ and in the transversal direction $x + y = \text{constant}$.

E. Working along the diagonal

To study in more detail the behaviour of such a function in this zone one can perform a Taylor expansion of $F(x, y)$ around $x = y$.

$$\lim_{x \rightarrow y} \frac{\tilde{W}_\nu(x, y)}{(x - y)} \equiv \lim_{x \rightarrow y} \frac{\begin{vmatrix} J_\nu(x) & J_\nu(y) \\ x J'_\nu(x) & y J'_\nu(y) \end{vmatrix}}{(x - y)} \quad (94)$$

$$= \lim_{x \rightarrow y} \frac{\begin{vmatrix} J_\nu(x) & J_\nu(x) + (x - y)J'_\nu(x) \\ x J'_\nu(x) & x J'_\nu(x) + (x - y)[J'_\nu(x) + x J''_\nu(x)] \end{vmatrix}}{(x - y)} \quad (95)$$

$$= \begin{vmatrix} J_\nu(x) & J'_\nu(x) \\ x J'_\nu(x) & J'_\nu(x) + x J''_\nu(x) \end{vmatrix} \quad (96)$$

$$= J_\nu(x)[J'_\nu(x) + x J''_\nu(x)] - x J'_\nu(x)^2. \quad (97)$$

The derivatives can be eliminated by using the well known recursion relations.

$$\lim_{x \rightarrow y} \frac{\tilde{W}_\nu(x, y)}{(x - y)} = J_\nu(x) \left[\frac{(\nu^2 - x^2)}{x} \right] - x \left[\frac{\nu}{x} J_\nu(x) - J_{\nu+1}(x) \right]^2 \quad (98)$$

$$= 2\nu J_\nu(x) J_{\nu+1}(x) - x [J_\nu^2(x) + J_{\nu+1}^2(x)]. \quad (99)$$

For sake of simplicity we shall use an equivalent form of Eq. (99) where lower order Bessel function appear

$$\lim_{x \rightarrow y} \frac{\tilde{W}_\nu(x, y)}{(x - y)} = 2\nu J_\nu(x) J_{\nu-1}(x) - x [J_\nu^2(x) + J_{\nu-1}^2(x)]. \quad (100)$$

This result shows that, as expected, each term of $F(x, x)$ is finite along the diagonal and equal to zero at $x = y = 0$. Moreover

$$D(x) \equiv F(x, x) = \sum_{l=1}^{\infty} (2l + 1) \frac{\{(2l + 1)J_{l+1/2}(x)J_{l-1/2}(x) - x [J_{l+1/2}^2(x) + J_{l-1/2}^2(x)]\}^2}{4x^2}. \quad (101)$$

This sum can easily be checked to be convergent for fixed x . [Use Eq. (90).] With a little more work it can be shown that

$$\lim_{x \rightarrow \infty} D(x) = \frac{1}{2\pi^2}.$$

The truncated function obtained after summation over the first few terms (say the first ten or so terms) is a long and messy combination of trigonometric functions that can however be easily plotted and approximated in the range of interest. Due to numerical artifacts, the function is not controllable near the origin, fortunately we have analytic information in that region — the function is very near to zero in the range $(0, 1)$ for both “out” and “in” frequencies, and can be approximated by zero without any undue influence on the numerical results. A semi-analytical study led us to the approximate form of $D(x)$

$$D(x) \approx \Theta(x - 1) \frac{1}{2\pi^2} \frac{2(x - 1)^2}{3 + 2(x - 1)^2}. \quad (102)$$

A confrontation between the two curves in the range of interest is given in the figure below.

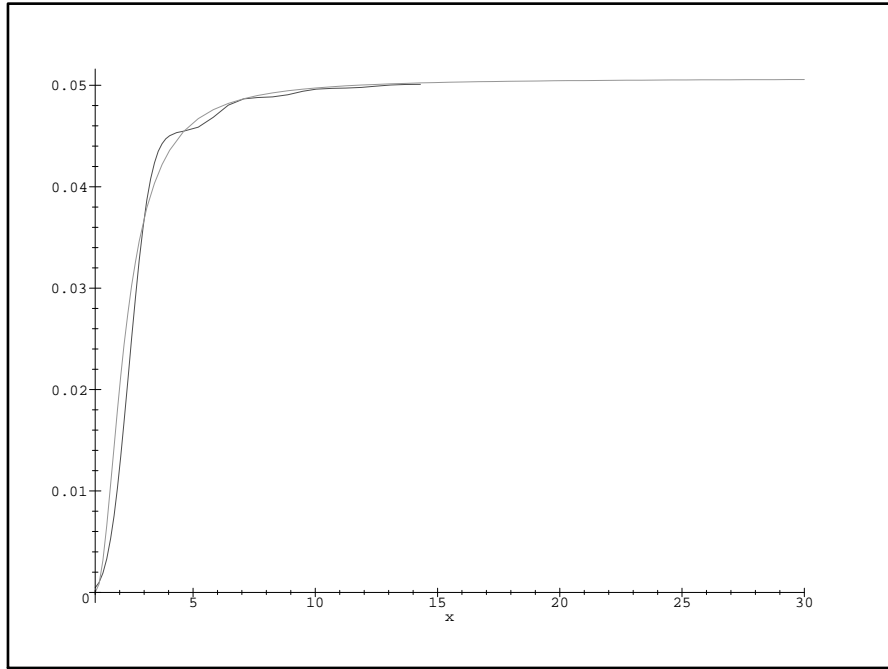


FIG. 2. Plot of the exact $D(x)$ against its approximated form in the range $1 < x < 30$

F. The factorization approximation

To numerically perform the integrals needed to do obtain the spectrum it is useful to note the approximate factorization property

$$F(x, y) \approx F\left(\frac{x+y}{2}, \frac{x+y}{2}\right) G\left(\frac{x-y}{2}\right). \quad (103)$$

That is: to a good approximation $F(x, y)$ is given by its value along the nearest part of the diagonal, multiplied by a universal function of the distance away from the diagonal. A little experimental curve fitting is actually enough to show that to a good approximation

$$F(x, y) \approx D\left(\frac{x+y}{2}\right) \frac{\sin^2(\pi[x-y]/4)}{(\pi[x-y]/4)^2}. \quad (104)$$

From the plot we show below it is easy to check that the function $F(x, y)$ is quite well fitted by our approximation. We feel important to stress that this is approximation is based on numerical experimentation, and is not an analytically-driven approximation. (In the infinite volume case we know that $F(x, y) \rightarrow (\text{constant}) \times \delta(x-y)$, *cf.* Eq. (70). The effect of finite volume is effectively to “smear out” the delta function. The combination $\sin^2(x)/(\pi x^2)$ is one of the standard approximations to the delta function.) Our approximation is quite good everywhere except for values of x and y near the origin (less than 1) where the contribution of the function to the integral is very small.

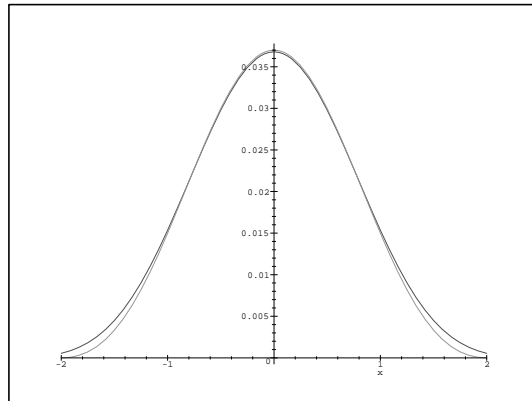


FIG. 3. Transverse fit: An orthogonal slice of $F(x, y)$ intersecting the diagonal at $(x, y) = (3, 3)$. Here $F(3 + z, 3 - z)$ is plotted in comparison with $[\sin^2(\pi z/2)]/(\pi z/2)^2$.

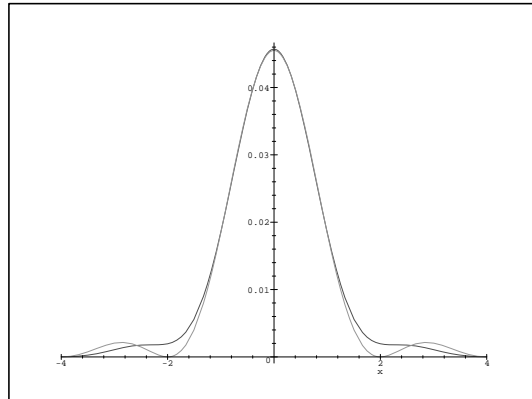


FIG. 4. Transverse fit: An orthogonal slice of $F(x, y)$ intersecting the diagonal at $(x, y) = (5, 5)$. Here $F(5 + z, 5 - z)$ is plotted in comparison with $[\sin^2(\pi z/2)]/(\pi z/2)^2$.

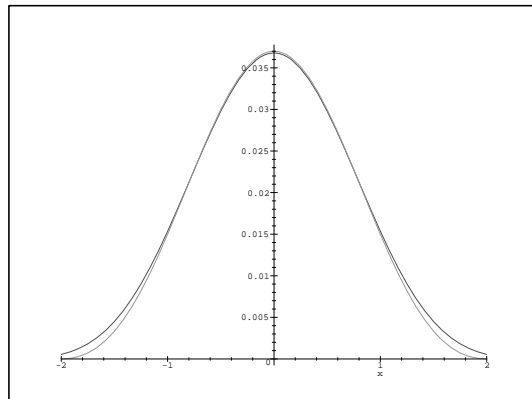


FIG. 5. Transverse fit: An orthogonal slice of $F(x, y)$ intersecting the diagonal at $(x, y) = (10, 10)$. Here $F(10 + z, 10 - z)$ is plotted in comparison with $[\sin^2(\pi z/2)]/(\pi z/2)^2$.

G. The spectrum: numerical evaluation

We have now transformed the function $F(x, y)$ into an easy to handle product of two functions

$$F(x, y) \approx \Theta(x + y - 2) \frac{1}{2\pi^2} \frac{(x + y - 2)^2}{6 + (x + y - 2)^2} \frac{\sin^2(\pi[x - y]/4)}{(\pi[x - y]/4)^2}. \quad (105)$$

We exhibit tridimensional graphs for both the exact (apart from the approximation of truncating the sum at a finite l) and approximate forms of the function $F(x, y)$. We have chosen the case of $R = 0.5\mu\text{m}$ (corresponding to $y_{max} = 2.5$ as previously explained).

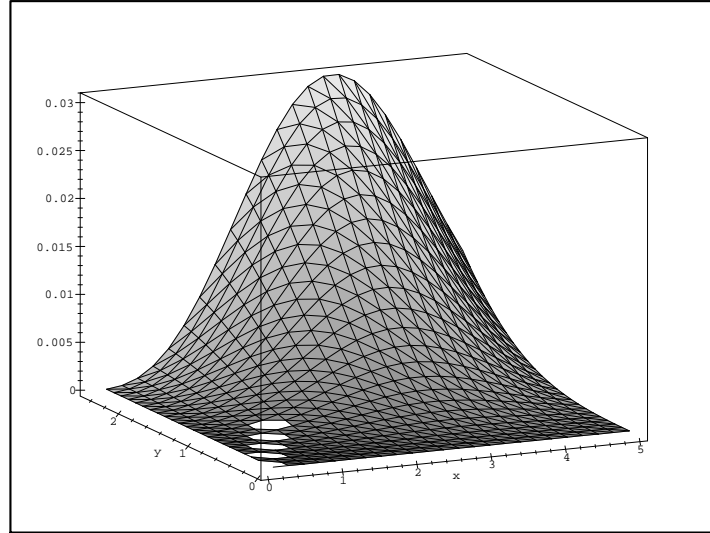


FIG. 6. Plot of the exact $F(x, y)$ in the range $0 < x < 5$, $0 < y < 2.5$

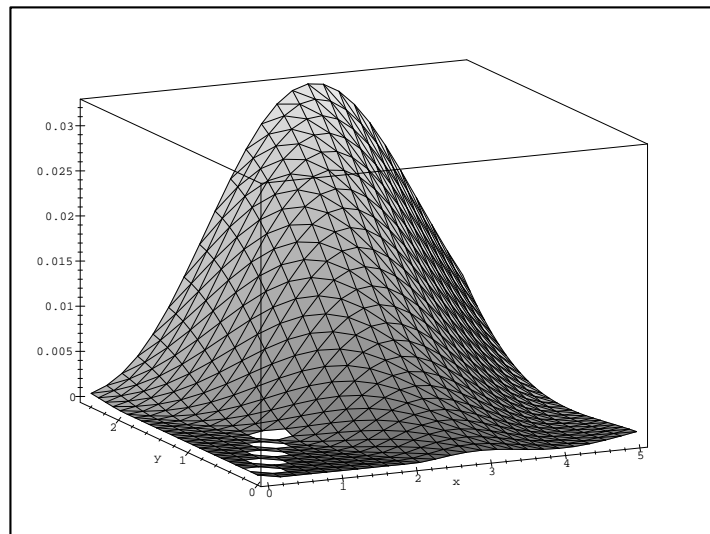


FIG. 7. Plot of the approximated $F(x, y)$ in the range $0 < x < 5$, $0 < y < 2.5$

A numerical study of the error due to the replacement of $F(x, y)$ with its approximated form Eq. (105), leads to an upper limit of 20% error in the total energy emitted. The dimensionless spectrum, based on Eqs. (52) and (87), is

$$\frac{dN}{dx} = \frac{(n_{liquid}^2 - n_{gas}^2)^2}{n_{liquid}^3 n_{gas}^3} \int_0^{RK} \left(\frac{y^2}{n_{gas} x + n_{liquid} y} \right)^2 D\left(\frac{x+y}{2}\right) \frac{\sin^2(\pi[x-y]/4)}{(\pi[x-y]/4)^2} dy. \quad (106)$$

As a consistency check, the infinite volume limit is equivalent to making the formal replacements

$$\frac{\sin^2(\pi[x-y]/4)}{(\pi[x-y]/4)^2} \rightarrow 4\delta(x-y), \quad (107)$$

and

$$D\left(\frac{x+y}{2}\right) \rightarrow \frac{1}{2\pi^2}. \quad (108)$$

Doing so, Eq. (106) reduces to Eq. (78) up to an overall factor $[4/\pi]$ of order one. The correct dependence on refractive index and correct power-law behaviour for the spectrum are recovered, and the overall order one factor is merely a reflection of the crudity of the cutoff in angular momentum used in deriving (78).

With this consistency check out of the way, it is now possible to perform the integral with respect to y to estimate the spectrum for finite volume. For definiteness we set $n_{liquid} = 1.3$ and $n_{gas} = 1.0$, put $K = 1/(200nm)$, and pick $R = 0.5\mu\text{m}$ (corresponding to $y_{max} = 2.5$). We integrate from $y = 0$ to $y = 2.5$ and plot the resulting spectrum from $x = 0$ to $x = 6$.

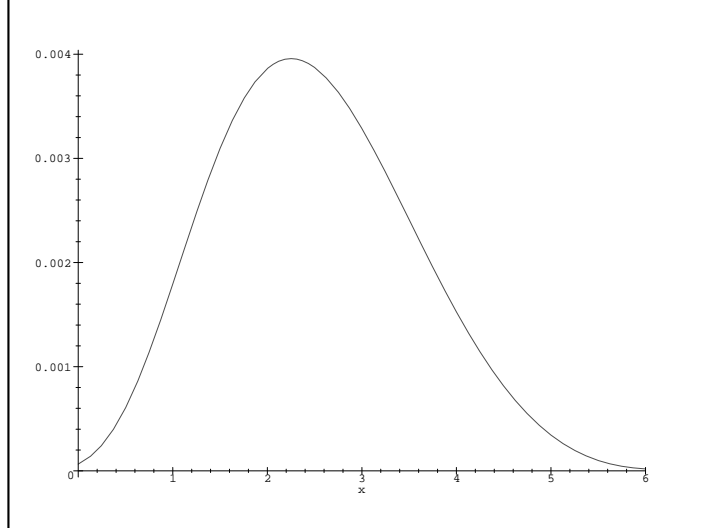


FIG. 8. Spectrum obtained by the approximated Bogolubov coefficient for $R = 0.5\mu\text{m}$ corresponding to $y_{max} = 2.5$. We integrate from $y = 0$ to $y = 2.5$ and plot the resulting spectrum from $x = 0$ to $x = 6$.

One can also ask what sort of result one would get if instead we pick a much larger value of R , say $R = 5\mu\text{m}$, corresponding to the bubble at equilibrium radius. In this case the approach towards the Schwinger (infinite volume result) result is much closer. We now have $y_{max} = 25$. We integrate from $y = 0$ to $y = 25$ and plot the resulting spectrum from $x = 0$ to $x = 35$. For comparison we plot it together with Eq. (78) which is Schwinger's naive model (the re-scaled infinite volume limit).

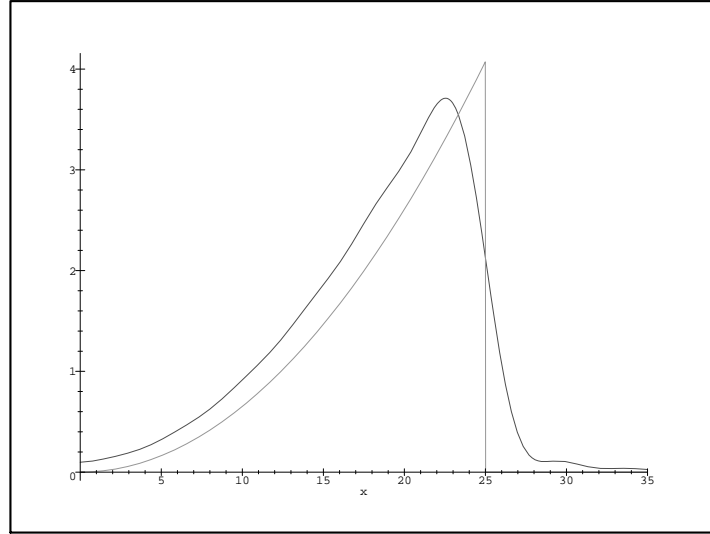


FIG. 9. Spectrum obtained by the approximated Bogolubov coefficient for $R = 5\mu\text{m}$ corresponding to $y_{max} = 25$. We integrate from $y = 0$ to $y = 25$ and plot the resulting spectrum from $x = 0$ to $x = 35$.

Finally, if we pick $R = 50\mu\text{m}$, corresponding to the bubble at maximum radius, we have $y_{max} = 250$. We integrate from $y = 0$ to $y = 250$ and plot the resulting spectrum from $x = 0$ to $x = 350$.

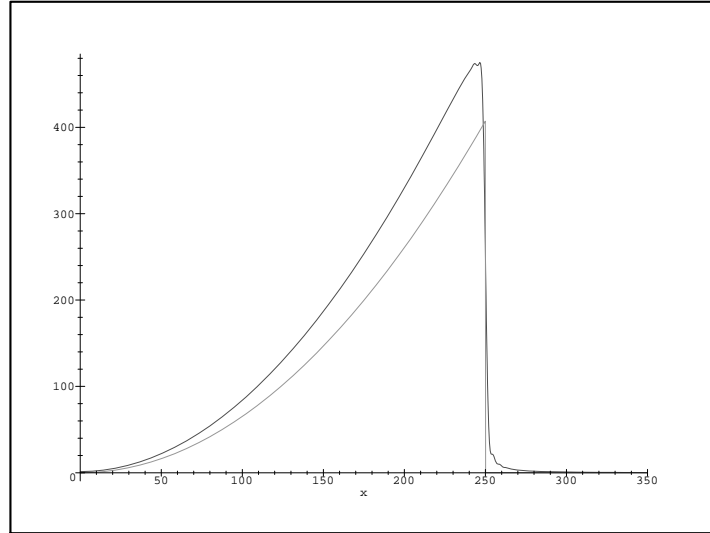


FIG. 10. Spectrum obtained by the approximated Bogolubov coefficient for $R = 50\mu\text{m}$ corresponding to $y_{max} = 250$. We integrate from $y = 0$ to $y = 250$ and plot the resulting spectrum from $x = 0$ to $x = 350$.

IV. CONCLUSIONS

The present paper presents calculations of the Bogolubov coefficients relating the two QED vacuum states appropriate to the collapse of a dielectric bubble. We have verified by explicit computation that photons are produced in bubble collapse, and are in agreement with Schwinger that QED vacuum effects remain a viable candidate for explaining SL.

Of course, the present model is not a complete theory: presently we can relate only the asymptotic “in” states to the asymptotic “out” states via these Bogolubov coefficients. A complete theory of SL will need to address specific timing information (when does the flash occur, what is its duration?), the role of noble gas admixtures, and dependence on ambient temperature, all of which the present simplified model does not yet address. We suspect that the phenomenon of parametric resonance may play an important role, in which case dynamical aspects of the bubble collapse cannot be idealized away.

Additionally, in Schwinger’s original model the bubble contents were simply approximated by air at STP (so that the dielectric properties of the bubble itself were approximated by vacuum). We also suspect that this approximation will have to be replaced by a more precise model for the dielectric properties of the bubble contents in order to build models capable of fitting detailed spectral and timing information.

Another lesson learned from this paper is that in order that the conversion of zero-point fluctuations to real photons be relevant for sonoluminescence we would want the sudden approximation to hold for photons all the way out to the cutoff (200nm; corresponding to a period of 0.66×10^{-15} sec). That’s a *femtosecond* timescale. This implies that if conversion of zero-point fluctuations to real photons is a significant part of the physics of sonoluminescence then the refractive index must be changing significantly on femtosecond timescales. *Thus the changes in refractive index cannot be just due to the motion of the bubble wall.* (The bubble wall is moving at most at Mach 4 [1], for a 1 μ m bubble this gives a collapse timescale of 10^{-10} seconds, about 100 picoseconds.) In this regard, the comments of Yablonovitch [23] are particularly useful. Yablonovitch points out that, for instance, sudden ionization of a gas can lead to substantial changes in the refractive index on the sub-picosecond timescale. In fact, with a little trickery the “wavefront” for the changing refractive index can move at speeds exceeding that of light. (No physical particles move faster than light, but the phase boundary can move faster than light.)

This suggests a slightly different physical model from Schwinger’s original suggestion: Certainly the Casimir energy changes as the bubble collapses, but it is only in the sudden approximation that we can justify converting all the change in Casimir energy to real photons. We thus suggest that one should not be focussing on the actual collapse of the bubble, but rather the way in which the refractive index changes as a function of space and time: as the bubble collapses the gasses inside are compressed, and although the refractive index for air (plus noble gas contaminants) is 1 at STP it should be no surprise to see the refractive index of the trapped gas undergoing major changes during the collapse process.

Nevertheless, the present calculation (limited though it may be) represents an important advance: There now can be no doubt that bubble collapse (and the associated change in Casimir energy) leads to production of real photons—the controversial issues now move to quantitative ones of fitting the observed experimental data. We are hopeful that more detailed models and data fitting will provide better explanations of the details of the SL effect, and specifically wish to assert that models based on the QED vacuum remain viable.

ACKNOWLEDGEMENTS

This research was supported by the Italian Ministry of Science (DWS, SL, and FB), and by the US Department of Energy (MV). MV particularly wishes to thank SISSA (Trieste, Italy) for hospitality during closing phases of this research. DWS and SL wish to thank E. Tosatti for useful discussion. SL wishes to thank M. Bertola and B. Bassett for comments and suggestions.

APPENDIX: CONVERTING ZERO-POINT FLUCTUATIONS TO REAL PHOTONS

In this appendix we describe a simple analytically tractable model for the conversion of zero point fluctuations (Casimir energy) into real photons. The model describes the effects of a time-dependent refractive index in the infinite volume limit. We show that for sudden changes in the refractive index the conversion of zero-point fluctuations is highly efficient, being limited only by phase space, whereas adiabatic changes of the refractive index lead to exponentially suppressed photon production.

1. Defining the model

Take an infinite homogeneous dielectric with a permittivity $\epsilon(t)$ and a permeability $\mu(t)$ that depend only on time, not on space. The $dF = 0$ Maxwell equations are

$$B = \nabla \times A; \quad (\text{A1})$$

$$E = -\nabla\phi - \frac{1}{c} \frac{\partial A}{\partial t}; \quad (\text{A2})$$

while the source-free $*d * F = 0$ Maxwell equations become

$$\nabla \cdot (\epsilon E) = 0; \quad (\text{A3})$$

$$\nabla \times \left(\frac{B}{\mu} \right) = +\frac{1}{c} \frac{\partial}{\partial t} (\epsilon E). \quad (\text{A4})$$

Substituting into this last equation

$$\nabla \times \left(\frac{1}{\mu} \nabla \times A \right) = -\frac{1}{c} \frac{\partial}{\partial t} \left[\epsilon \left(\nabla\phi + \frac{1}{c} \frac{\partial A}{\partial t} \right) \right]. \quad (\text{A5})$$

Suppose that $\mu(t)$ and $\epsilon(t)$ depend on time but not space, then

$$\frac{1}{\mu} (\nabla(\nabla \cdot A) - \nabla^2 A) = -\nabla \frac{1}{c} \frac{\partial}{\partial t} (\epsilon\phi) - \frac{1}{c^2} \frac{\partial}{\partial t} \epsilon \frac{\partial A}{\partial t}. \quad (\text{A6})$$

Pick a *generalized* Lorentz gauge to simplify life

$$\frac{1}{\mu} \nabla \cdot A + \frac{1}{c} \frac{\partial}{\partial t} (\epsilon\phi) = 0. \quad (\text{A7})$$

Then the equations of motion reduce to

$$\frac{1}{c^2} \frac{\partial}{\partial t} \epsilon \frac{\partial A}{\partial t} = \nabla^2 A. \quad (\text{A8})$$

We now introduce a fake “pseudo-time” parameter by defining

$$\frac{\partial}{\partial \eta} = \epsilon(t) \frac{\partial}{\partial t}. \quad (\text{A9})$$

That is

$$\eta(t) = \int \frac{dt}{\epsilon(t)}. \quad (\text{A10})$$

In terms of this fake time parameter the equation of motion is

$$\frac{\partial^2}{\partial \eta^2} A = c^2 \frac{\epsilon(\eta)}{\mu(\eta)} \nabla^2 A. \quad (\text{A11})$$

Now pick a convenient profile for the permittivity and permeability as a function of fake time. (This choice of time profile for the refractive index makes the problem analytically tractable, with a little more work it is possible to consider generic monotonic changes of refractive index and place bounds on the Bogolubov coefficients.) Let’s take

$$\frac{\epsilon(\eta)}{\mu(\eta)} = a + b \tanh(\rho\eta). \quad (\text{A12})$$

Of course, this profile has been picked so that we can solve the differential equations exactly. For instance (with a few minor changes of notation) we can just write down the answers directly from pages 60–62 of Birrell and Davies [28].

(Birrell and Davies were interested in the problem of particle production engendered by the expansion of the universe in a cosmological context. Although the physical model is radically different here the mathematical aspects of the analysis carry over with some minor translation in the details.) Equations (3.88) of Birrell-Davies become

$$\omega_{in} = k\sqrt{a-b} = k\sqrt{\frac{\epsilon_{in}}{\mu_{in}}} = k\tilde{n}_{in} = k\frac{n_{in}}{\mu_{in}}; \quad (\text{A13})$$

$$\omega_{out} = k\sqrt{a+b} = k\sqrt{\frac{\epsilon_{out}}{\mu_{out}}} = k\tilde{n}_{out} = k\frac{n_{out}}{\mu_{out}}; \quad (\text{A14})$$

$$\omega_{\pm} = \frac{1}{2}k(\tilde{n}_{in} \pm \tilde{n}_{out}). \quad (\text{A15})$$

The Bogolubov β coefficients can be copied down from Birrell-Davies (3.92)

$$\beta(\vec{k}_{in}, \vec{k}_{out}) = \sqrt{\frac{\omega_{out}}{\omega_{in}} \frac{\Gamma(1 - i\omega_{in}/\rho)\Gamma(i\omega_{out}/\rho)}{\Gamma(i\omega_{+}/\rho)\Gamma(1 + i\omega_{-}/\rho)}} \delta^3(\vec{k}_{in} - \vec{k}_{out}). \quad (\text{A16})$$

Birrell and Davies suppress the delta function but it's easy enough to convince yourself it's there. Now square, using Birrell-Davies (3.95). We obtain

$$|\beta(\vec{k}_{in}, \vec{k}_{out})|^2 = \frac{\sinh^2(\pi\omega_{-}/\rho)}{\sinh(\pi\omega_{in}/\rho)\sinh(\pi\omega_{out}/\rho)} \frac{V}{(2\pi)^3} \delta^3(\vec{k}_{in} - \vec{k}_{out}). \quad (\text{A17})$$

We now consider two limits, the adiabatic limit and the sudden limit and see what happens.

2. Sudden limit:

Take

$$\rho \gg \max\{\omega_{in}, \omega_{out}, \omega_{+}, \omega_{-}\}. \quad (\text{A18})$$

This corresponds to a rapidly changing refractive index. Then

$$|\beta|^2 \propto \frac{(\pi\omega_{-}/\rho)^2}{(\pi\omega_{in}/\rho)(\pi\omega_{out}/\rho)}. \quad (\text{A19})$$

More precisely

$$|\beta(\vec{k}_{in}, \vec{k}_{out})|^2 \approx \frac{1}{4} \frac{(\omega_{in} - \omega_{out})^2}{\omega_{in}\omega_{out}} \frac{V}{(2\pi)^3} \delta^3(\vec{k}_{in} - \vec{k}_{out}), \quad (\text{A20})$$

We can re-write this directly in terms of the change in the “refractive index” as

$$|\beta(\vec{k}_{in}, \vec{k}_{out})|^2 \approx \frac{1}{4} \frac{(\tilde{n}_{in} - \tilde{n}_{out})^2}{\tilde{n}_{in}\tilde{n}_{out}} \frac{V}{(2\pi)^3} \delta^3(\vec{k}_{in} - \vec{k}_{out}), \quad (\text{A21})$$

This result is exactly that obtained in the body of this paper when we considered the large-volume limit for dielectric bubbles in order to reproduce the original Schwinger estimate of photon production [2–8]. It should also be compared to the discussion of Yablonovitch [23] [see particularly the formulae in the paragraph between equations (8) and (9)].

3. Adiabatic limit:

Take

$$\rho \ll \min\{\omega_{in}, \omega_{out}, \omega_+, \omega_-\}. \quad (\text{A22})$$

This corresponds to a slowly changing refractive index. Then

$$|\beta|^2 \propto \frac{\exp(2\pi\omega_-/\rho)}{\exp(\pi\omega_{in}/\rho) \exp(\pi\omega_{out}/\rho)}. \quad (\text{A23})$$

More precisely

$$|\beta(\vec{k}_{in}, \vec{k}_{out})|^2 \approx \exp(-2\pi\omega_{out}/\rho) \frac{V}{(2\pi)^3} \delta^3(\vec{k}_{in} - \vec{k}_{out}), \quad (\text{A24})$$

This implies exponential suppression of photon production for frequencies large compared to ρ . (Eberlein's model [9–11] for sonoluminescence explicitly makes the adiabatic approximation and this effect is the underlying reason why photon production is so small in that model; of course the technical calculations of that model also include the finite volume effects due to finite bubble radius which somewhat obscures the underlying physics of the adiabatic approximation.)

4. Spectrum:

The number spectrum of the emitted photons is

$$\frac{dN(\vec{k}_{out})}{d^3\vec{k}_{out}} = \left(\int |\beta(\vec{k}_{in}, \vec{k}_{out})|^2 d^2\vec{k}_{in} \right). \quad (\text{A25})$$

This easily yields

$$\frac{dN(\omega_{out})}{d\omega_{out}} = \frac{\sinh^2(\pi\omega_-/\rho)}{\sinh(\pi\omega_{in}/\rho) \sinh(\pi\omega_{out}/\rho)} \frac{V}{(2\pi)^3} \frac{4\pi\omega_{out}^2}{\tilde{n}_{out}^3}. \quad (\text{A26})$$

For low frequencies (where the sudden approximation is valid) this is a phase-space limited spectrum with a prefactor that depends only on the overall change of “refractive index”. For high frequencies (where the adiabatic approximation holds sway) the spectrum is cutoff in an exponential manner depending on the rapidity of the change in refractive index. A sample spectrum is plotted in figure 11. For comparison figure 12 shows a Planckian spectrum with the same exponential falloff at high frequencies, while the two curves are superimposed in figure 13.

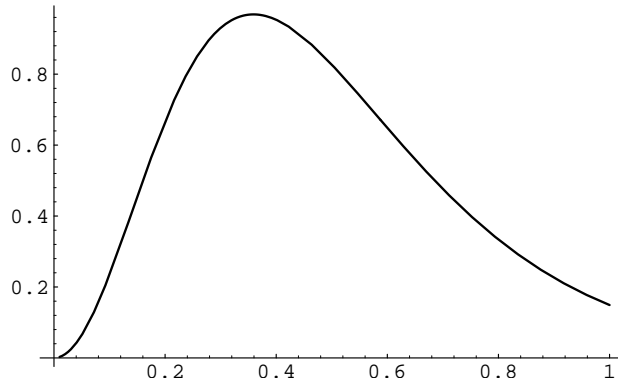


FIG. 11. Number spectrum (photons per unit frequency and volume) for $\tilde{n}_{in} = 2$, $\tilde{n}_{out} = 1$. The horizontal axis is ω_{out}/ρ . The vertical axis is in arbitrary units.

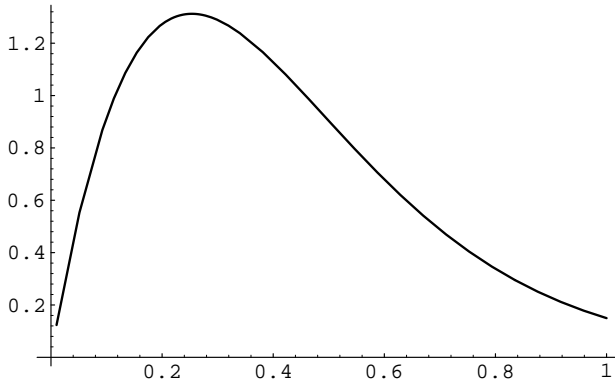


FIG. 12. Number spectrum for a Planck blackbody curve with $kT/\equiv 2\pi\rho$. The horizontal axis is ω_{out}/ρ . The vertical axis is in arbitrary units (but with the same normalization as figure 1).

5. Bounds:

One might worry that the results of this appendix are specific to the choice of profile (A12). That the results are more general can be established by analyzing general bounds on the Bogolubov coefficients: We shall here quote only the key result that for any monotonic change in the dielectric parameters the sudden approximation provides a strict upper bound on the magnitude of the Bogolubov coefficients. A proof of this statement will be deferred for another paper [29].

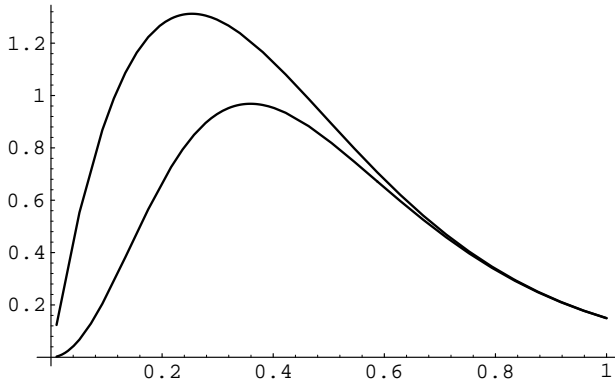


FIG. 13. Superimposed number spectra. Showing similar high-frequency behaviour although low energy behaviour is different (quadratic versus linear).

6. Discussion:

Lesson 1: This is only a toy model, but we feel it adequately proves that efficient photon production occurs only in the sudden approximation, and that photon production is suppressed in the adiabatic regime. The particular choice of profile $\epsilon(\eta)$ was merely a convenience, it allowed us to get analytic exact results, but it's not a critical part of the analysis.

Lesson 2: Eberlein's model for sonoluminescence [9–11] explicitly uses the adiabatic approximation. For arbitrary adiabatic changes we expect the exponential suppression to still hold with ρ now being some measure of the timescale over which the refractive index changes.

Lesson 3: Schwinger's model for sonoluminescence [2–8] implicitly uses the sudden approximation. It is only for the sudden approximation that we recover Schwinger's phase-space limited spectrum. For arbitrary changes the sudden approximation provides a rigorous upper bound on photon production.

In summary, it is only in the sudden approximation that efficient conversion of zero-point fluctuations to real photons takes place. Though this result is derived here only for a particularly simple toy model we expect this part of the analysis to be completely generic. We expect that any mechanism for converting zero-point fluctuations to real photons will exhibit similar effects.

[†] E-mail: liberati@sissa.it

[‡] E-mail: belgiorno@mi.infn.it

[¶] E-mail: visser@kiwi.wustl.edu

[§] E-mail: sciama@sissa.it

- [1] B.P. Barber, R.A. Hiller, R. Löfstedt, S.J. Putterman Phys. Rep. **281**, 65-143 (1997).
- [2] J. Schwinger, Proc. Nat. Acad. Sci. **89**, 4091–4093 (1992).
- [3] J. Schwinger, Proc. Nat. Acad. Sci. **89**, 11118–11120 (1992).
- [4] J. Schwinger, Proc. Nat. Acad. Sci. **90**, 958–959 (1993).
- [5] J. Schwinger, Proc. Nat. Acad. Sci. **90**, 2105–2106 (1993).
- [6] J. Schwinger, Proc. Nat. Acad. Sci. **90**, 4505–4507 (1993).
- [7] J. Schwinger, Proc. Nat. Acad. Sci. **90**, 7285–7287 (1993).
- [8] J. Schwinger, Proc. Nat. Acad. Sci. **91**, 6473–6475 (1994).
- [9] C. Eberlein, *Sonoluminescence as quantum vacuum radiation*, Phys. Rev. Lett. **76**, 3842 (1996). quant-ph/9506023
- [10] C. Eberlein, *Theory of quantum radiation observed as sonoluminescence*, Phys. Rev. A **53**, 2772 (1996). quant-ph/9506024
- [11] C. Eberlein, *Sonoluminescence as quantum vacuum radiation (reply to comment)*, Phys. Rev. Lett. **78**, 2269 (1997). quant-ph/9610034
- [12] C. E. Carlson, C. Molina-París, J. Pérez-Mercader, and M. Visser, Phys. Lett. B **395**, 76-82 (1997). hep-th/9609195
- [13] C. E. Carlson, C. Molina-París, J. Pérez-Mercader, and M. Visser, Phys. Rev. D **56**, 1262 (1997). hep-th/9702007.
- [14] C. Molina-París and M. Visser, Phys. Rev. D **56**, 6629 (1997). hep-th/9707073.
- [15] B. Gompf, R. Günther, G. Nick, R. Pecha, and W. Eisenmenger, Phys. Rev. Lett. **78**, 1405 (1997).
- [16] R.A. Hiller, S.J. Putterman, and K.R. Weninger, Phys. Rev. Lett. **80**, 1090 (1998).
- [17] K. Milton, *Casimir energy for a spherical cavity in a dielectric: toward a model for Sonoluminescence?*, in *Quantum field theory under the influence of external conditions*, edited by M. Bordag, (Tuebner Verlagsgesellschaft, Stuttgart, 1996), pages 13–23. See also hep-th/9510091.
- [18] K. Milton and J. Ng, *Casimir energy for a spherical cavity in a dielectric: Applications to Sonoluminescence*, hep-th/9607186.
- [19] K. Milton and J. Ng, *Observability of the bulk Casimir effect: Can the dynamical Casimir effect be relevant to Sonoluminescence?*, hep-th/9707122.
- [20] P. Candelas, Ann. of Phys. **167**, 57-84 (1986)
- [21] I.H. Brevik, V.V. Nesterenko, and I.G. Pirozhenko, *Direct mode summation for the Casimir energy of a solid ball*, hep-th/9710101.
- [22] V.V. Nesterenko and I.G. Pirozhenko, *Is the Casimir effect relevant to sonoluminescence?*, hep-th/9803105,
- [23] E. Yablonovitch, Phys. Rev. Lett. **62**, 1742 (1989)
- [24] R. Schützhold, G. Plunien, and G. Soff, *Quantum radiation in external background fields*, quant-ph/9801035.
- [25] S. Liberati, M. Visser, F. Belgioro, and D.W. Sciama, *Sonoluminescence: Bogolubov coefficients for the QED vacuum of a collapsing bubble*, quant-ph/98mmnnn.
- [26] H. Bateman, *Higher Transcendental Functions*, Vol II, (McGraw-Hill, New York, 1953).
- [27] A. Jeffrey, *Handbook of Mathematical Formulas and Integrals*, page 219, (Academic Press, San Diego, 1995).
- [28] N.D. Birrell and P.C.W. Davies, *Quantum fields in curved space*, (Cambridge University Press, Cambridge, England, 1982).
- [29] M. Visser, in preparation.